

AWARD NUMBER: W81XWH-15-1-0137

TITLE: Photo-Acoustic Ultrasound Imaging to Distinguish Benign from Malignant Prostate Cancer

PRINCIPAL INVESTIGATOR: Michael Sano

CONTRACTING ORGANIZATION: Stanford University
Palo Alto, CA 94304-1212

REPORT DATE: September 2016

TYPE OF REPORT: Annual

PREPARED FOR: U.S. Army Medical Research and Materiel Command
Fort Detrick, Maryland 21702-5012

DISTRIBUTION STATEMENT: Approved for Public Release;
Distribution Unlimited

The views, opinions and/or findings contained in this report are those of the author(s) and should not be construed as an official Department of the Army position, policy or decision unless so designated by other documentation.

REPORT DOCUMENTATION PAGE				Form Approved OMB No. 0704-0188	
Public reporting burden for this collection of information is estimated to average 1 hour per response, including the time for reviewing instructions, searching existing data sources, gathering and maintaining the data needed, and completing and reviewing this collection of information. Send comments regarding this burden estimate or any other aspect of this collection of information, including suggestions for reducing this burden to Department of Defense, Washington Headquarters Services, Directorate for Information Operations and Reports (0704-0188), 1215 Jefferson Davis Highway, Suite 1204, Arlington, VA 22202-4302. Respondents should be aware that notwithstanding any other provision of law, no person shall be subject to any penalty for failing to comply with a collection of information if it does not display a currently valid OMB control number. PLEASE DO NOT RETURN YOUR FORM TO THE ABOVE ADDRESS.					
1. REPORT DATE September 2016		2. REPORT TYPE Annual		3. DATES COVERED 3Aug2015 - 2Aug2016	
4. TITLE AND SUBTITLE Photo-Acoustic Ultrasound Imaging to Distinguish Benign from Malignant Prostate Cancer				5a. CONTRACT NUMBER W81XWH-15-1-0137	
				5b. GRANT NUMBER	
				5c. PROGRAM ELEMENT NUMBER	
6. AUTHOR(S) Michael Sano E-Mail: mikesano@stanford.edu				5d. PROJECT NUMBER	
				5e. TASK NUMBER	
				5f. WORK UNIT NUMBER	
7. PERFORMING ORGANIZATION NAME(S) AND ADDRESS(ES) Stanford University Palo Alto, CA 94304-1212				8. PERFORMING ORGANIZATION REPORT NUMBER	
9. SPONSORING / MONITORING AGENCY NAME(S) AND ADDRESS(ES) U.S. Army Medical Research and Materiel Command Fort Detrick, Maryland 21702-5012				10. SPONSOR/MONITOR'S ACRONYM(S) USAMRMC	
				11. SPONSOR/MONITOR'S REPORT NUMBER(S)	
12. DISTRIBUTION / AVAILABILITY STATEMENT Approved for Public Release; Distribution Unlimited					
13. SUPPLEMENTARY NOTES					
14. ABSTRACT The aim of this project is to build a photoacoustic ultrasound imaging probe which can be deployed through the urethra to image the prostate from the inside out. Ultrasound imaging provides a basic view of the structure of the prostate while photoacoustic contrast is predicted to enhance our ability to discern benign from malignant tissues based on their vascular density. A prototype transurethral ultrasound probe has been constructed and preliminary photoacoustic experiments have been conducted to help predict the wavelengths in which imaging may be most effecting. The remainder of this project will be dedicated to incorporating photoacoustic capabilities onto the transurethral probe and evaluating the imaging system using tissue phantoms and animal models of disease.					
15. SUBJECT TERMS Photoacoustic, Ultrasound imaging, transurethral probe					
16. SECURITY CLASSIFICATION OF:			17. LIMITATION OF ABSTRACT Unclassified	18. NUMBER OF PAGES 15	19a. NAME OF RESPONSIBLE PERSON USAMRMC
a. REPORT Unclassified	b. ABSTRACT Unclassified	c. THIS PAGE Unclassified			19b. TELEPHONE NUMBER (include area code)

Table of Contents

	<u>Page</u>
1. Introduction.....	2
2. Keywords.....	2
3. Accomplishments.....	2
4. Impact.....	11
5. Changes/Problems.....	12
6. Products.....	12
7. Participants & Other Collaborating Organizations.....	13
8. Special Reporting Requirements.....	13
9. Appendices.....	13

1. **INTRODUCTION:**

Ultrasound imaging uses sound waves at frequencies above the human hearing range to image organs within the body. An ultrasound transducer delivers a pulse of acoustic energy into the area of interest and listens for the echoes which return as the sound waves bounce off of tissue structures in the body. Unfortunately, it is difficult to distinguish cancer from the surrounding healthy tissue. When tumors are visible, ultrasound images are unable to discriminate between benign or malignant cancers. In photoacoustic imaging, laser energy is transmitted into the tissue, absorbed, and an ultrasound wave is released. The wavelength (color) of the laser light can be adjusted to image specific structures within the tissue such as fat, blood vessels, or implanted metal objects. Unfortunately, laser energy cannot penetrate deep into the body and photoacoustic imaging of the entire prostate is not possible using an external laser source. Here, we propose to develop a photoacoustic ultrasound system which is small enough to travel up the urethra and image the prostate from the inside out. This will allow us to produce high resolution ultrasound images and distinguish between tumors which are poorly (benign) or excessively (malignant) vascularized.

2. **KEYWORDS:**

Photoacoustic (PA)

3. **ACCOMPLISHMENTS:**

What were the major goals of the project?

Major Training Task 1: Training and educational development in prostate cancer research (Months: 1 – 24)

Major Task 1: Characterize tumor prostate cancer phantom models (Months: 1 – 12)

Major Task 2: Build photoacoustic probe (Months 13-16)

Major Task 3: Characterize photoacoustic image reconstruction (Months 16-24)

What was accomplished under these goals?

Major Task 1: Characterization of Prostate Cancer Phantom Models

Specific Objective: Fabricate tumor mimicking prostate phantoms to determine the minimum contrast ratios of melanin and hemoglobin and determine the maximum resolution of prototypes.

Results, Developments, and Conclusions:

Prostate Mimicking Phantoms

The primary objective of this task was to develop prostate tissue phantoms which replicate the ultrasound and photo-thermal behavior of tissue including tumors. To accomplish this, a number of phantoms were constructed. The first replicated the mechanical physiology of the prostate with pathways replicating the urethra and seminal vesicle. The second was significantly larger than the prostate to test the maximum imaging depth of the prototype and included seven blank targets which could be filled with tumor mimicking material or metal objects. Finally, a square phantom with 16 targets was constructed to evaluate different melanin and hemoglobin concentrations using a commercial photoacoustic ultrasound probe.

Base phantom material was created by dissolving a 40 g/L concentration of sea plaque agarose into DI water heated to approximately 80°C. A 10 g/L concentration of silica powder was then added to mimic scattering properties of tissue and 3 g/L NaCl was added to increase the electrical conductivity of the phantom to a physiological level (~ 0.6 S/m). This base material was allowed to cool slightly, poured into a 3D printed mold while still viscous, and allowed to solidify overnight in a refrigerator.

Melanin and hemoglobin targets were created by first increasing the silica concentration in the base material to 40 g/L. This was done to enable ultrasound only visualization of the targets. Melanin targets replicating the pigment concentration in fair skin (0.011 mg/mL), medium skin (0.066 mg/mL), and dark skin (0.13 mg/mL) were created by first dissolving an appropriate amount of synthetic melanin powder into DI water then mixing the dissolved melanin into the silica/agarose material.

To compare the relative photoacoustic response of hemoglobin, equivalent molar weight concentrations of hemoglobin were evaluated: fair (6.16 μ M, 397 mg/L), medium (36.94 μ M, 2380 mg/L), and dark (72.76 μ M, 4690 mg/L). In addition, ‘fake blood’ targets were created by dissolving 58 g/L of hemoglobin into the silica/agarose material. It should be noted that normal hemoglobin levels in adult males range from 135 – 175 g/L, however, we were unable to successfully dissolve this concentration into the phantom material.

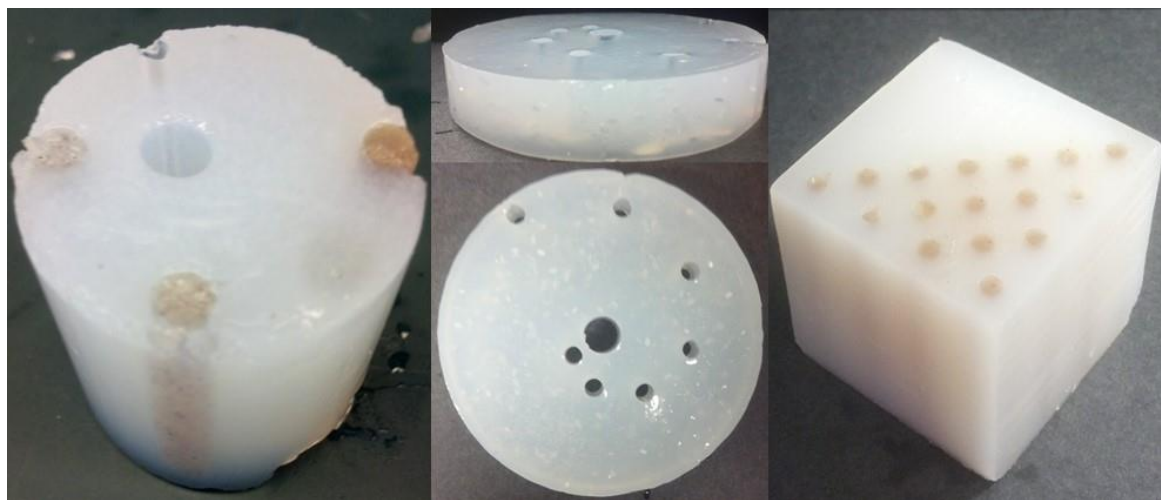


Figure 1: Prostate mimicking phantoms. (Left) Phantom replicating the relative size of the prostate including the urethra and seminal vesicle. (Center) Larger phantom with multiple target locations. (Right) Cube phantom for evaluating melanin and hemoglobin targets using a commercial ultrasound system.

Imaging of phantoms using a commercial system

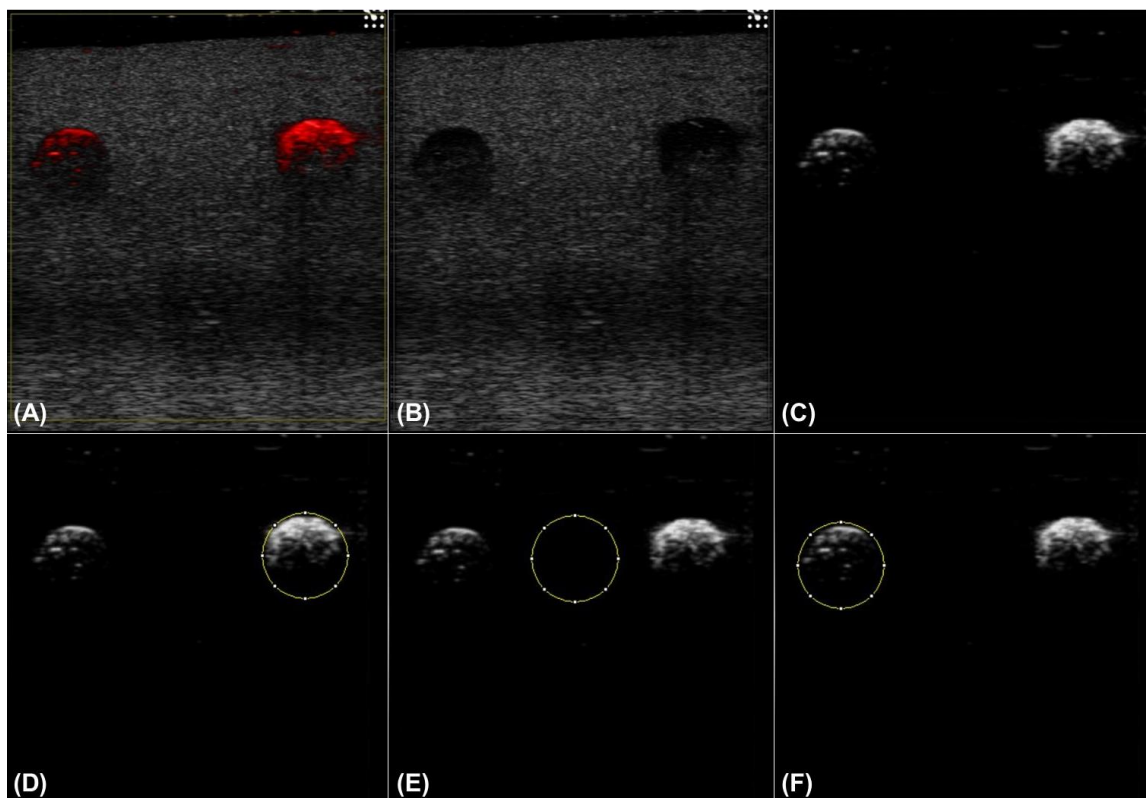


Figure 2: Photoacoustic images of prostate phantoms. (A) Combined photoacoustic and ultrasound image. (B) Ultrasound only image. (C) Photoacoustic only image. ImageJ was used to quantify the photoacoustic signal in the (D) right target [blood hemoglobin], (E) center control region, and (F) left target [dark melanin].

The relative photoacoustic signals from hemoglobin and melanin targets was initially evaluated using a VisualSonics Vevo 2100 ultrasound unit with a Vevo LAZR photo-acoustic imaging attachment. This system uses 20 or 50 MHz ultrasound array transducers equipped with fiberoptic probes to irradiate samples with pulsed laser light between 680 and 970 nm. A 20 MHz array was used to image all phantoms as the 50 MHz transducer was unable to image targets beyond approximately 1 cm from the surface. In each experiment, two adjacent targets were imaged at wavelengths between 680 and 960 nm in 5 nm increments (Figure 2A). A minimum of 6 acquisitions were made for each target. The frames were exported from the ultrasound system in AVI movie format and imported into VirtualDub (1.10.4, Avery Lee) where individual frames were extracted and saved as JPEG files. Each frame was individually imported into ImageJ (1.48, NIH, Bethesda, MD) and split into red, green, and blue channels. The raw ultrasound data in the blue channel (Figure 2B) was subtracted from the image to obtain the photoacoustic data (Figure 2C). Pixel intensity data in the right target (Figure 2D), control region (Figure 2E), and left target (Figure 2F) were then measured and normalized by dividing the mean pixel value in each region of interest by 255 (the maximum value if all pixels were illuminated).

Regions containing light, medium, and dark skin melanin concentrations exhibited some degree of photoacoustic contrast at all wavelengths between 680 and 960 nm (Figure 3, Figure 4). Light skin melanin contrast targets had speckled regions of contrast mostly concentrated near the top surface of the target (Figure 5). Darker melanin targets had a PA response which spanned the entire target for most wavelengths (Figure 5). However, the equivalent molecular weight hemoglobin targets did not produce significant PA contrast at these wavelengths. The fake blood hemoglobin targets were visible across the entire spectrum. The photoacoustic intensity of light skin melanin targets was relatively flat between 680 and 960 nm. Medium skin and dark skin targets had successively higher PA intensities which appeared to decrease as the wavelength increased. The light, medium, and dark hemoglobin targets exhibited essentially no PA response across the entire spectrum. The fake blood targets, however, had a higher PA response than the dark and medium melanin targets below 785 and 885 nm, respectively (Figure 4B,D). The fake

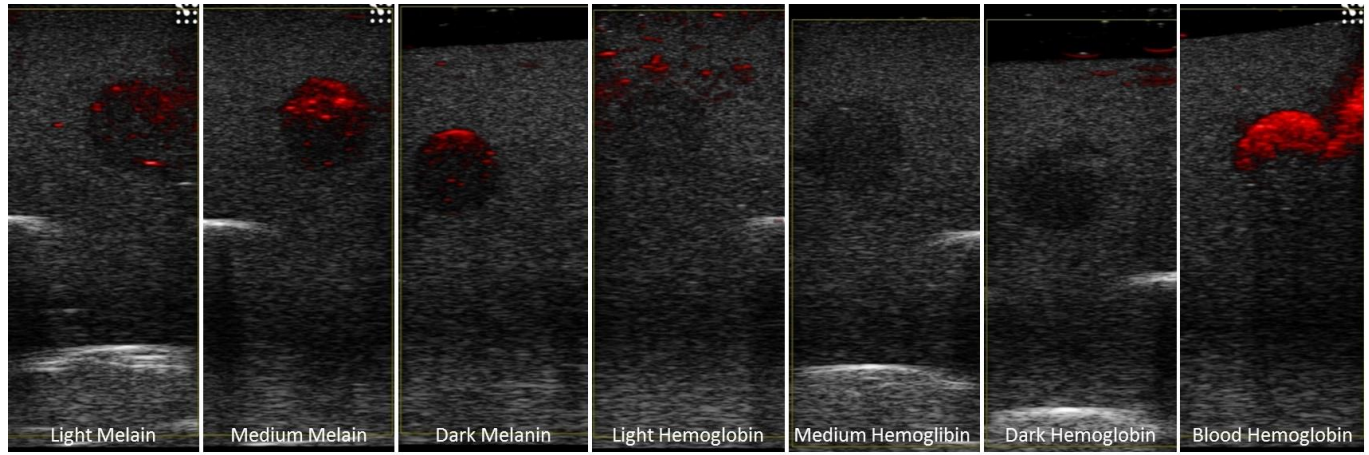


Figure 3: Photoacoustic response of hemoglobin and melanin targets at 680nm.

blood target had a higher PA response than the light skin melanin target for all wavelengths investigated. **These results indicate that some degree of PA contrast between pigmented skin and highly vascularized tissue may be possible.**

Challenges with Photoacoustic Imaging Using Intrinsic Contrast

This study found two potential challenges which will inhibit imaging deep seated tumors using photoacoustic contrast: 1) over absorption in high contrast targets and 2) penetration depth of short wavelengths. PA imaging of fake blood targets (Figure 5A-C) resulted in hemispherical regions of high PA contrast rather than contrast within the entire circular target region. These hemispherical regions occurred on the top surface of the target nearest the laser light source and resulted from the near complete absorption of the incident light by the proximal regions of the target. These regions of high contrast effectively shield the remaining target and prevent accurate imaging of the entire volume.

Imaging of targets centered 7.5 mm below the surface (5.0 – 10 mm, Figure 7B) was easily achieved using PA contrast. However, when targets centered 15 mm below the surface (12.5 – 17.5 mm, Figure 7B) produced nearly no PA contrast. Quantitatively,

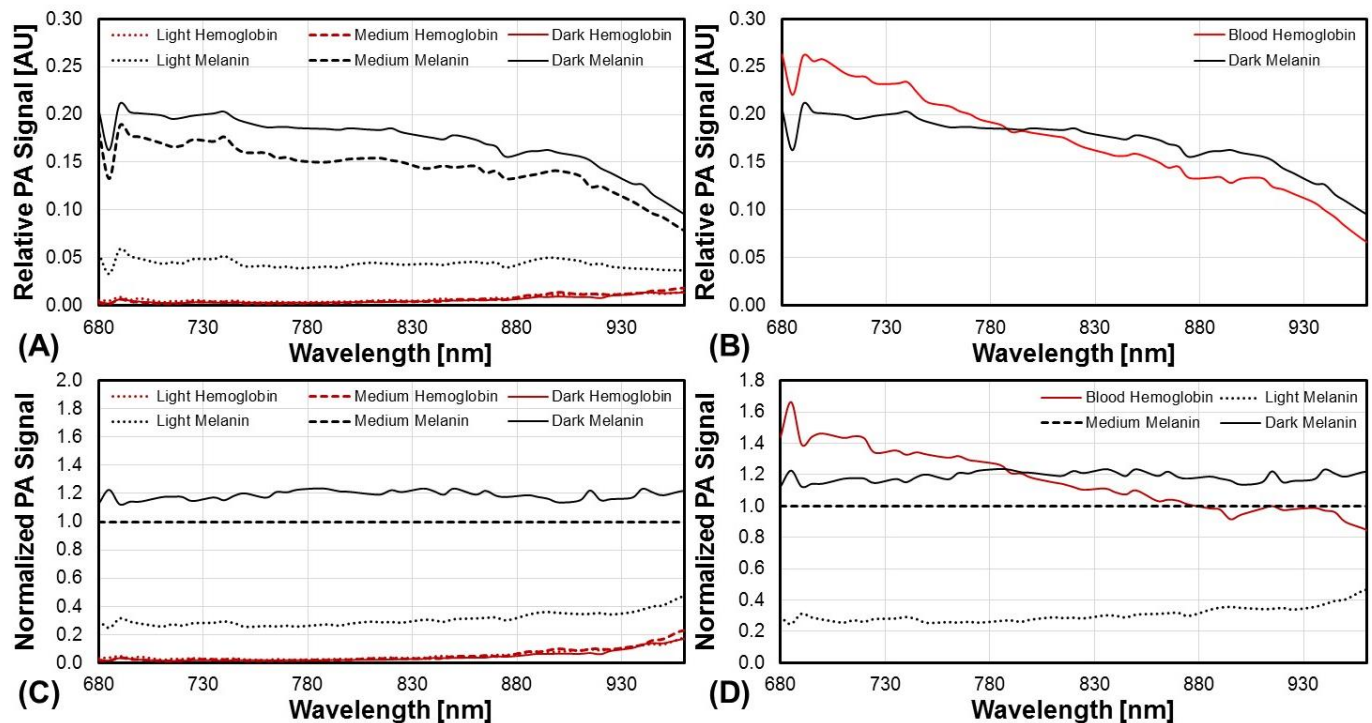


Figure 4: Wavelength response of hemoglobin and melanin targets. (A) Relative photoacoustic response of equivalent molecular weight hemoglobin and melanin targets. (B) Photoacoustic response of dark melanin and ‘fake blood’ hemoglobin target. Responses of (C) equivalent molecular weight targets and (D) ‘fake blood’ targets normalized to the ‘medium melanin’ target signal.

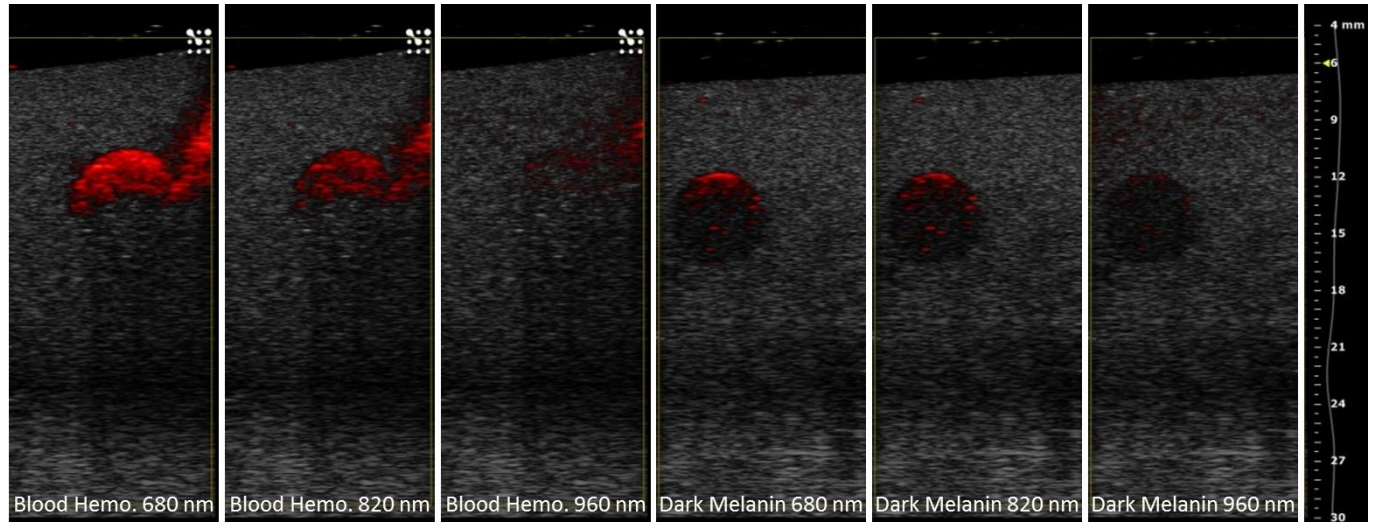


Figure 5: Wavelength response of blood hemoglobin and dark melanin targets. Blood hemoglobin PA contrast is more intense than dark melanin targets at lower wavelengths indicating that some degree of PA contrast is possible in pigmented tissues.

over the entire wavelength spectrum the targets 7.5 mm below the surface produced 17 – 64 times more photoacoustic contrast ($41x \pm 15x$) than the targets which were 15 mm below the surface. Qualitatively, the targets 15 mm below the surface were indistinguishable from background noise independent of the gain settings used.

These measurements and observations indicate that there may be significant challenges with imaging deep seated or irregularly shaped tumors, however, these results may also be the result of the relatively rigid software tools available on the commercial PA ultrasound system used and customized data acquisition and image reconstruction techniques may be more capable of imaging these types of targets in combination with application specific PA ultrasound probes designed for transurethral imaging of the prostate.

Discussion of Goals Not Met

Determination of the absolute minimum resolution of photoacoustic targets was challenging using commercial ultrasound transducers. Targets with hemoglobin concentrations similar to whole blood were easily identifiable. However, light was not able to fully penetrate these targets resulting in hemispherical regions of PA contrast within a known circular target. In contrast, a circular geometry was visible using PA contrast for targets with lower hemoglobin targets, but these targets will potentially be obscured in pigmented tissues. The use of sophisticated mean and weighted image construction algorithms may enhance our

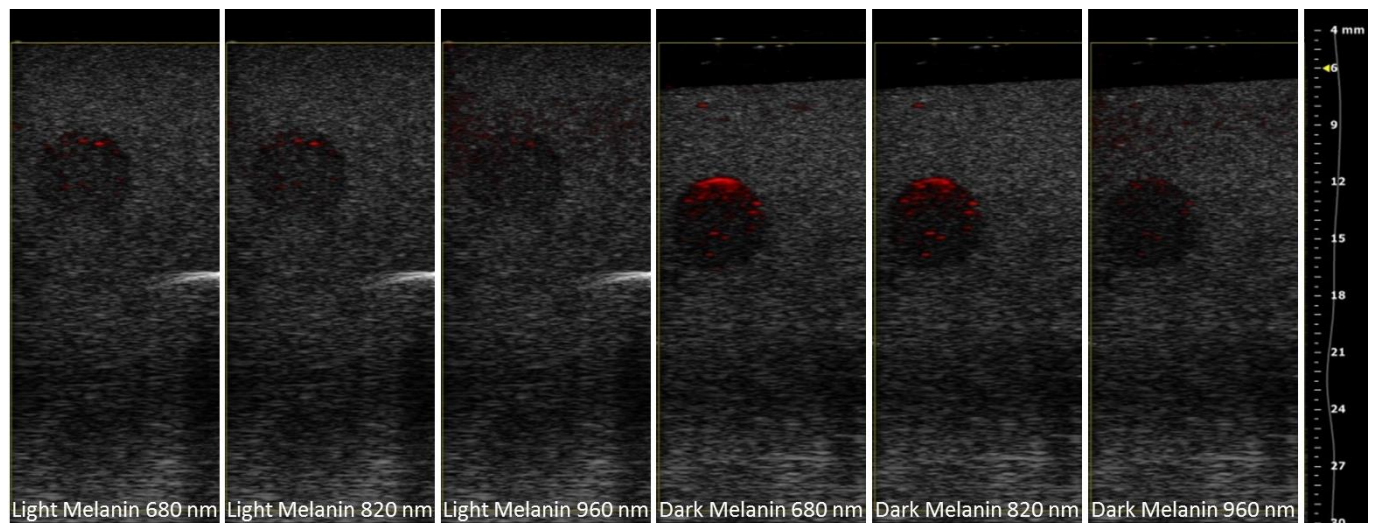


Figure 6 Wavelength response of melanin targets.

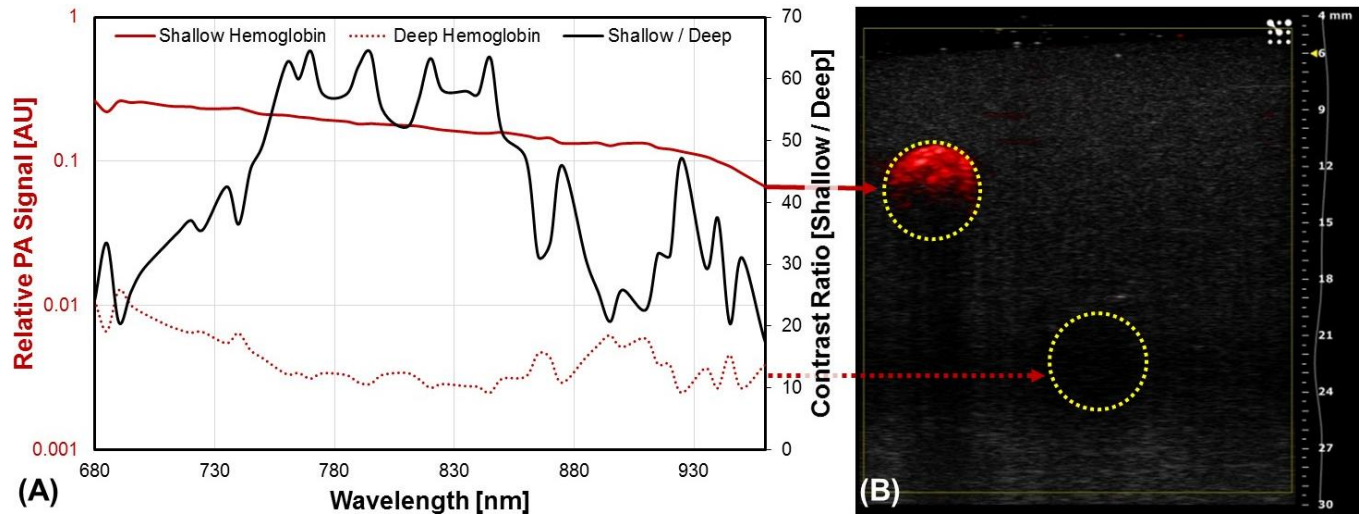


Figure 7: Challenges with deep tissue imaging.

ability to resolve small targets, however, we do not have access to raw RF data from the commercial systems to evaluate these techniques. We are developing custom data acquisition and image reconstruction software for the transurethral probe which will enable the use of more sophisticated techniques.

Major Task 2: Build Photoacoustic Probe (Months 13-16)

Specific Objectives: Assemble photoacoustic transducer and build motorized controls to rotate sensor assembly.

A two stage approach was taken in the fabrication of the transurethral PA ultrasound probe. First, we built and validated an ultrasound only probe capable of being deployed through the urethra. In the second year of this grant fiber optic light delivery will be added to the probe and PA contrast recognition software will be developed.

Results, Developments, and Conclusions:

A single element 20 MHz ultrasound transducer (Biatek Inc.) was embedded in a 3D printed probe body (Figure 8). A soft polymer adhesive was used as a backing material to secure the transducer in place and make the electrical connections water tight. The coaxial cables were attached to a custom circuit board and routed to a 50 Ω BNC connector. A commercial ultrasound pulser and receiver was used to drive the single element. The output signal from the probe was amplified and routed through a custom PCB into a high speed data acquisition system (Analog Discovery, Digilent Inc., Pullman, WA).

Custom ultrasound reconstruction software (Figure 10A) was written in Python to control the data acquisition hardware and motor used to rotate the sample. Briefly, individual A-line scans were acquired at 100 MSPS in 8000 sample blocks. For each A-line one or more sample blocks were captured and the data was averaged and weighted. Once an A-line was acquired, the

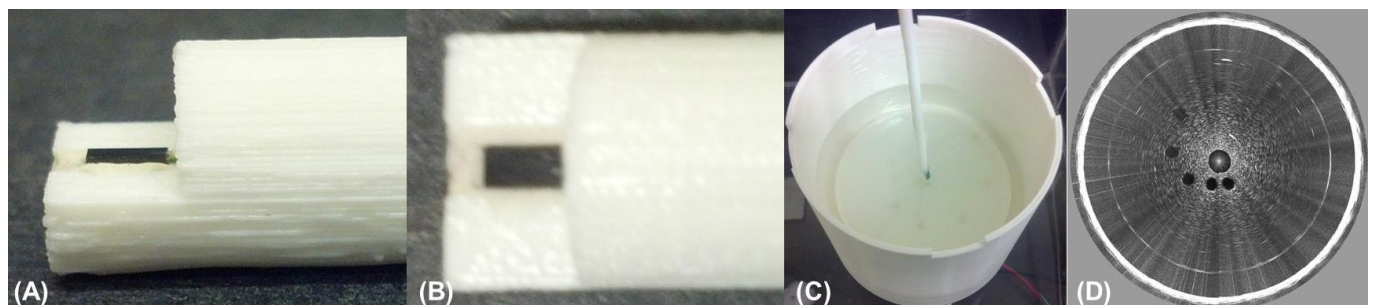


Figure 8: Transurethral ultrasound probe. (A) Side view and (B) top down view of the single element ultrasound probe embedded in a 3D printed probe body. (C) Imaging of phantom in a rotating water tank which revolves the sample around the probe body. (D) Deconstructed ultrasound image of the phantom.

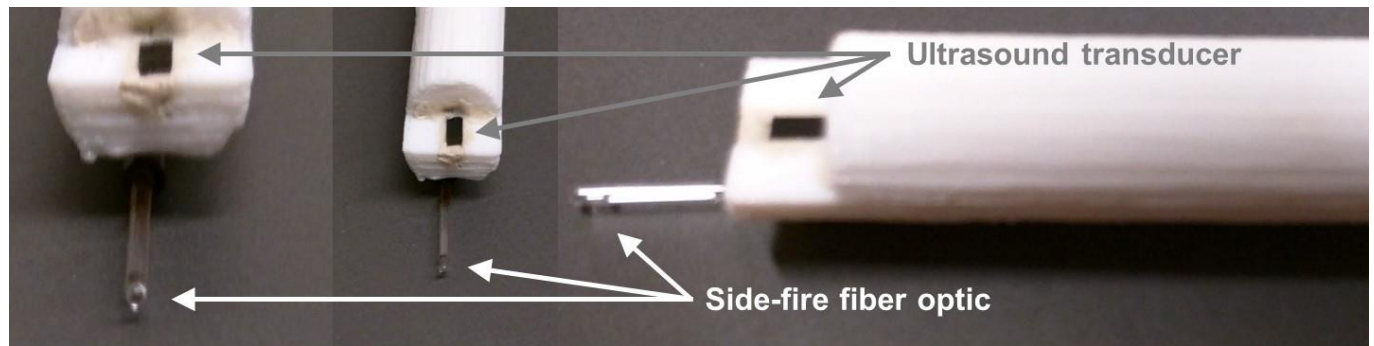


Figure 9: Transurethral photoacoustic probe with side-fire fiber optic assembly.

motor was rotated by one step, approximately 0.1-1 degree, and the process was repeated. Each A-line was projected into cylindrical coordinates to generate an ultrasound image.

Discussion of Goals Not Met

This major task (Months 13 – 16) is nearly completed and on schedule. A transurethral ultrasound probe has been designed and tested without photoacoustic imaging capabilities. In the next 12 months, the fiber optics required for photoacoustic contrast imaging will be incorporated into the probe. Software for initiating laser pulses and recording the photoacoustic signal will be written and an additional toolbox for adding photoacoustic contrast on top of the ultrasound image will be created.

Major Task 3: Characterize Photoacoustic Image Reconstruction (Months 16 – 22)

Specific Objectives: Program data acquisition and image reconstruction algorithms to image phantoms. Use photoacoustic prototype to image animal models of disease.

As with Major Task 2, this was broken into two components. First, software for image construction of ultrasound only images was created for use with the transurethral probe. This component has been completed. Second, software for adding photoacoustic image contrast onto the ultrasound image will be developed; this component is development.

Results, Developments, and Conclusions:

A number of strategies were employed to optimize the acquisition and reconstruction of the ultrasound images. To tune these strategies a simple prostate mimicking phantom (Figure 10 B-C) was used which included seven empty 5 mm targets evenly spaced between 1 cm and 4 cm from the center of the phantom. The primary strategy employed was A-line sample averaging in which multiple samples were acquired for each probe orientation and averaged. This technique drastically increased the signal to noise ratio in the images and also served to eliminate random noise from the stepper motor controller. Other techniques

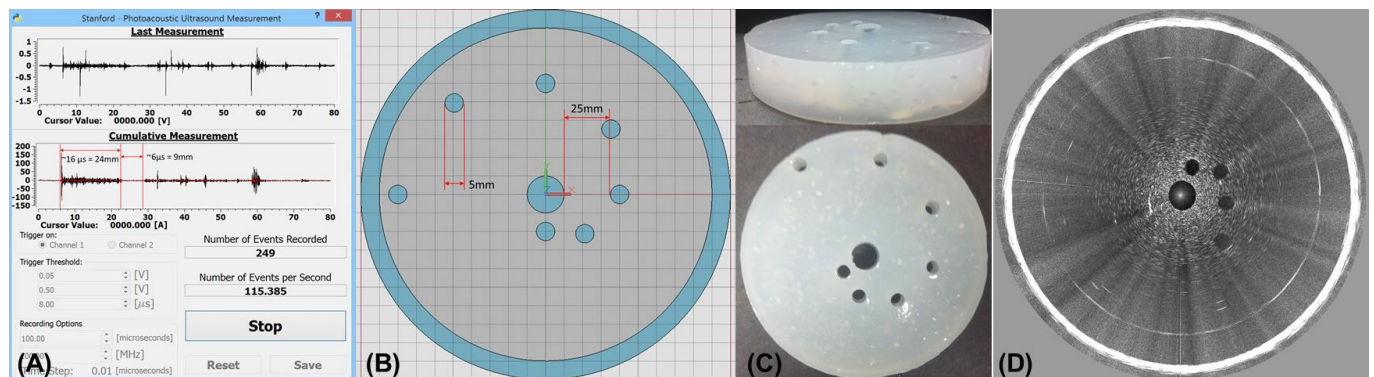


Figure 10: Image reconstruction software and calibration phantom. (A) Custom software written to control the ultrasound acquisition and motor control hardware. (B) Schematic layout and (C) actual phantom used for designing and calibrating the acquisition software. (D) Image reconstructed with 50 samples per A-line.

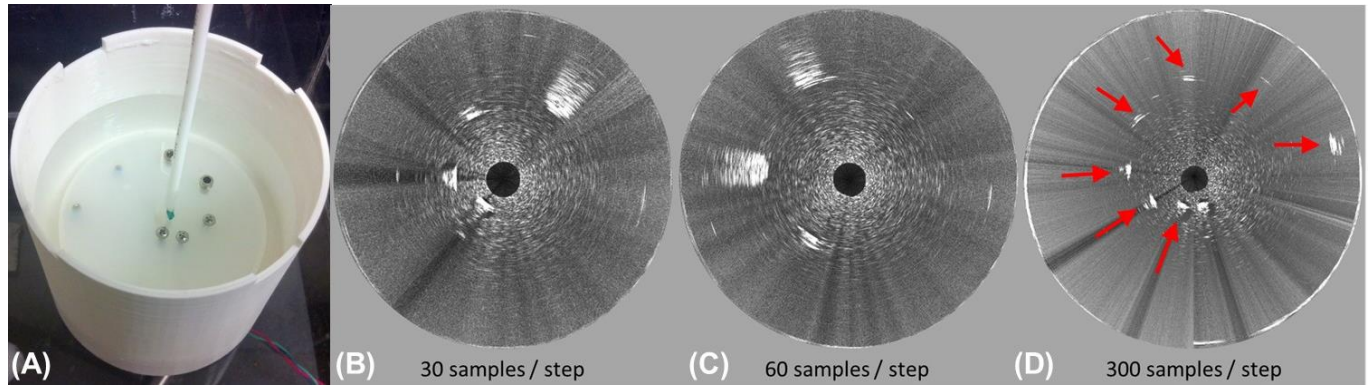


Figure 11: Image reconstruction and metal target localization strategies. (A) Prostate mimicking phantom with metal objects embedded at known locations. Images generated using stochastic reflection reduction technique which acquired and averaged an increasing number of samples per A-line before rotating the phantom. Images were generated after acquiring (B) 30 samples, (C) 60 samples, and (D) 300 samples per A-line.

included rectifying and normalizing the A-line data and progressive amplification of signals as a function of their offset from the image origin. Sample averaging had the largest observable effect on image quality, but also significantly increased the image acquisition time as samples could only be acquired at approximately 100 A-lines per second. However, changes to the data acquisition hardware could significantly improve this acquisition rate, minimizing the overall acquisition time to an acceptable duration.

A major benefit of A-line sample averaging is that this drastically reduces scattering noise from metal objects in the imaging field. This reduction in noise allows for better localization of targets as shown in Figure 11. Increasing the number of samples per A-line from 30 to 300 significantly reduced scattering noise from metal objects placed in the calibration target (Figure 11B, D). **This technique may be useful for needle placement during biopsy or in focal cancer treatments where accurate placement is critical.**

The A-line sample averaging technique also worked for imaging soft targets. Figure 12 shows a similar calibration phantom in which the voids were filled with highly scattering targets with varying concentrations of hemoglobin. An acceptable ultrasound image is obtained using only a single A-line sample per step (Figure 12B), however, increasing the number of samples to 2 (Figure 12C), 5 (Figure 12D), and 10 (Figure 12E) helped to improve the signal to noise ratio. Fewer samples are needed per A-line because the soft targets are not as highly scattering as metal objects and are more easily resolved.

A number of direct comparisons between commercially available ultrasound probes and the transurethral ultrasound probe are shown in Figures 13 and 14. A phantom mimicking the approximate geometry of the prostate including the urethra and seminal

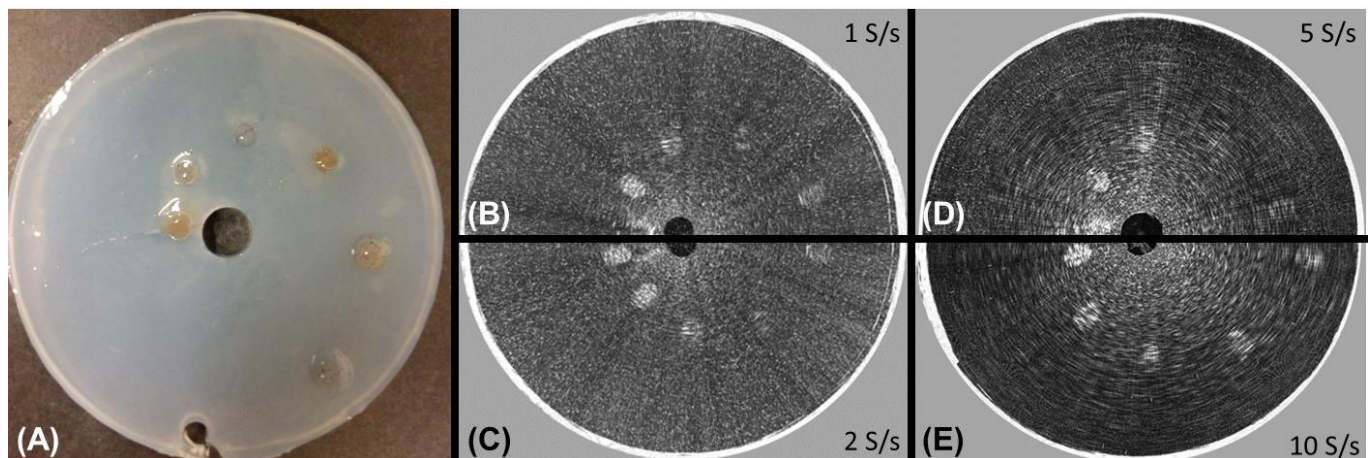


Figure 12: Image reconstruction of scattering PA targets. (A) 19 cm diameter prostate mimicking phantom with highly scattering hemoglobin target material. Images generated with an increasing number of samples per A-line before rotating the phantom. Images were generated after acquiring (B) 1 sample, (C) 2 samples, (D) 5 samples, and (E) 10 samples per A-line.

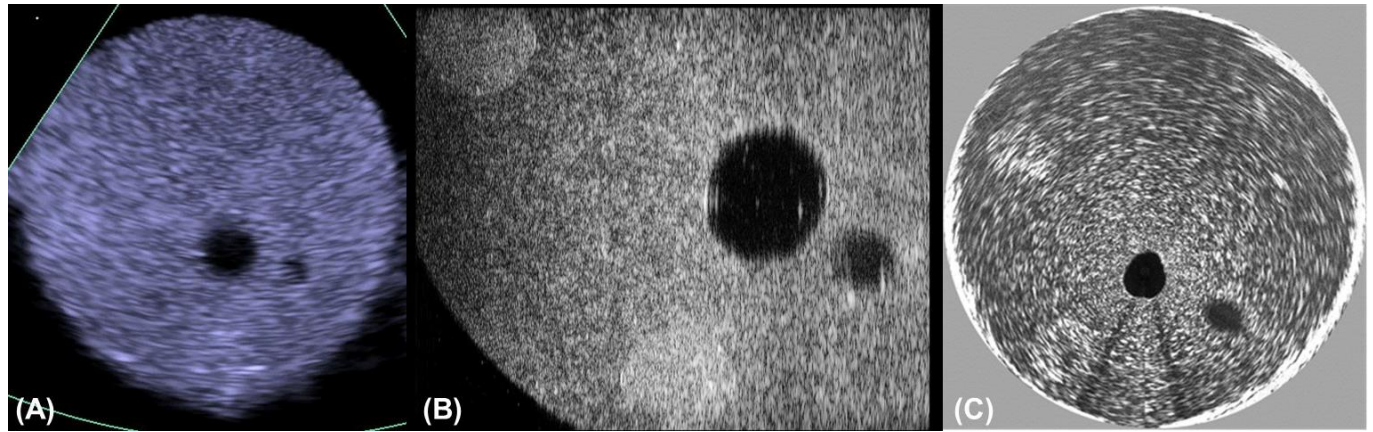


Figure 13: Comparison of transurethral probe with commercial transducers. Images acquired with (A) an 8 MHz intravenous (IVUS) ultrasound probe, (B) a 20 MHz hand held transducer, and (C) the transurethral ultrasound probe developed in this project. The transurethral probe has higher image contrast than the IVUS probe and a larger field of view than the hand held transducers.

vesicle (Figure 13) was imaged using an 8 MHz commercial intravenous ultrasound system (IVUS, Figure 13A), a commercial 20 MHz hand held ultrasound transducer array (VevoSonics, Figure 13B), and the transurethral ultrasound probe developed in this project (Figure 13C). The images from the IVUS probe are relatively low quality and highly scattering targets representing tumor tissue within the phantom are not visible. The image quality of the hand held transducer array is significantly improved above the IVUS probe, however, these transducers have a relatively shallow penetration depth and small field of view. The transurethral ultrasound probe is able to resolve the highly scattering targets as well as the entire phantom in a single image.

When larger phantoms were imaged (Figure 14), the large field of view of the transurethral probe becomes more obvious. The 20 MHz hand held ultrasound transducer is able to image targets which are approximately 10 mm from the transducer surface (Figure 14B), however, the transurethral probe is able to clearly resolve targets which are up to 17.5 mm from the probe surface. Additional fine tuning of the image reconstruction algorithms may eventually further improve this imaging depth. However, in its current iteration, the transurethral probe is currently able to resolve a total area of 9.6 cm^2 and should be capable of imaging the entire prostate volume.

Discussion of Goals Not Met

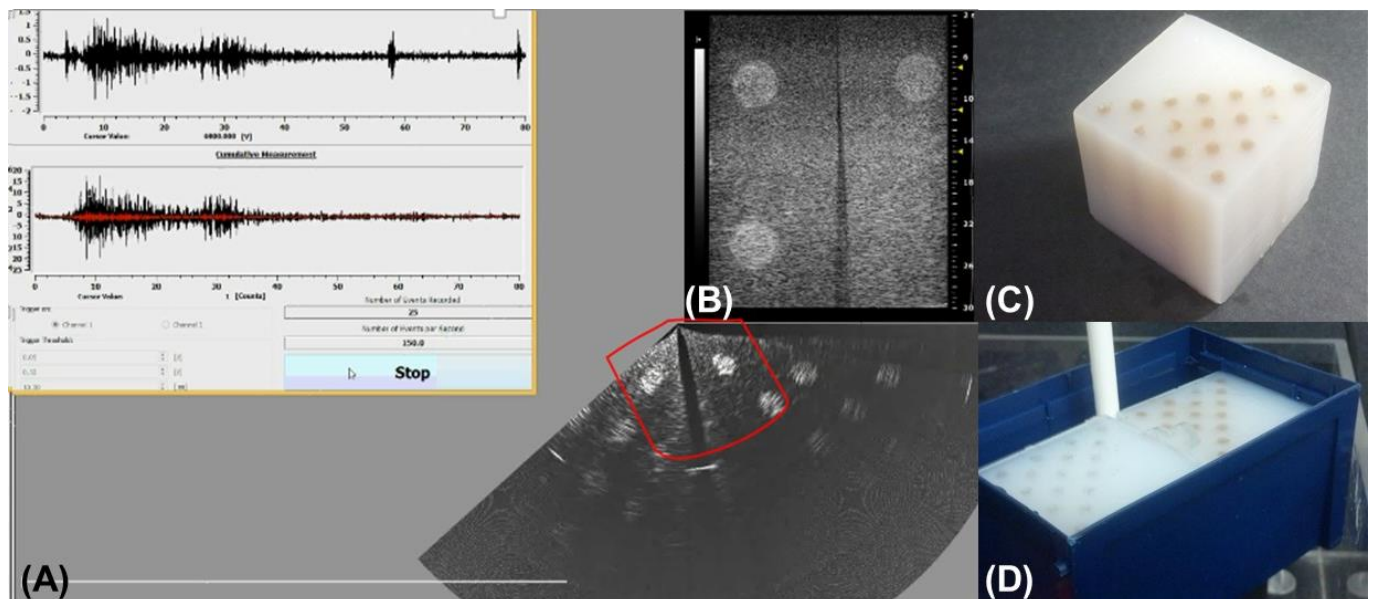


Figure 14: Comparison of transurethral probe with commercial transducers. Images acquired with (A) the transurethral probe developed in this project and (B) a commercial 20 MHz hand held transducer. The transurethral probe is capable of imaging a significantly larger field of view than commercial probes. The red outline in (A) approximates the field of view of the commercial 20 MHz probe within the image acquired by the transurethral probe. (C, D) Prostate mimicking phantoms with soft scattering targets with multiple hemoglobin concentrations.

This major task (Months 16 – 22) is on schedule. Data acquisition and image reconstruction software has been developed and tested without photoacoustic imaging capabilities. In the next 12 months, photoacoustic contrast image reconstruction will be incorporated into the software. Phantoms originally imaged only with ultrasound will be re-imaged with photoacoustic contrast and preliminary in-vivo experiments will be conducted.

What opportunities for training and professional development has the project provided?

The PI has audited a number of courses during this training period including INDE 231: Future Faculty Seminar and HRP 209: FDA's Regulation of Health Care. He will attend the AIChE conference to chair a session in the fall and will continue to attend regular meetings of the Stanford BioX program.

Through his participation in the Future Faculty Seminar, Dr. Sano submitted faculty applications to 27 universities, was invited for on-site interviews at five, and received four tenure track offers. He will begin a full time position at the UNC-NC State Department of Biomedical Engineering in 2017.

How were the results disseminated to communities of interest?

The results from this proposal were presented at weekly laboratory meetings as well as the annual meeting of the American Association of Physics in Medicine. Additional abstracts and journal publications are underway which are specifically focused on this work. In addition, Dr. Sano has had one manuscript accepted: *Production of Spherical Ablations using Non-Thermal Irreversible Electroporation* and has an additional two manuscripts in revisions.

What do you plan to do during the next reporting period to accomplish the goals?

During the next reporting period, we will finish building the photoacoustic probe and associated software, test the system on prostate mimicking phantoms, and evaluate the system on animal models of disease.

4. IMPACT:

What was the impact on the development of the principal discipline(s) of the project?

The PI has attended a number of seminars and classes to prepare him for an academic career. He is chairing a session at an upcoming conference and will continue to present his work at lab and department meetings. Through this training program, the PI has successfully interviewed for and received a tenure track faculty appointment in a program associated with a top 25 medical school and top 50 engineering program.

What was the impact on other disciplines?

This work will have a substantial impact on multiple disciplines including medical imaging, focal therapies, and medical diagnostics.

What was the impact on technology transfer?

Nothing to report

What was the impact on society beyond science and technology?

Nothing to report

5. **CHANGES/PROBLEMS:**

Changes in approach and reasons for change

Nothing to report

Actual or anticipated problems or delays and actions or plans to resolve them

Changes that had a significant impact on expenditures

Nothing to report

Significant changes in use or care of human subjects, vertebrate animals, biohazards, and/or select agents

Significant changes in use or care of human subjects

Nothing to report

Significant changes in use or care of vertebrate animals.

Nothing to report

Significant changes in use of biohazards and/or select agents

Nothing to report

6. **PRODUCTS:** *List any products resulting from the project during the reporting period. If there is nothing to report under a particular item, state "."*

Publications, conference papers, and presentations

Journal publications.

Michael B. Sano#, Richard Fan, Gloria Hwang, Geoffrey Sonn, Lei Xing - *Production of Spherical Ablations using Non-Thermal Irreversible Electroporation*, Journal of Vascular and Interventional Radiology, Vol 27, Issue 9, 2016, pages 1432-1440 e3, Published, acknowledgment of federal support: yes

Michael B. Sano#, Richard Fan, Lei Xing – *High Frequency Pulse Waveforms Affect Lethal Thresholds*, Nature Scientific Reports, Under Review, acknowledgment of federal support: yes

Michael B. Sano#, Olga Volotskova, Lei Xing – *Synergistic Effects of High Frequency Pulsed Electric Fields and X-Ray Irradiation*, IEEE Transactions on Biomedical Engineering, Under Review, acknowledgment of federal support: yes

Books or other non-periodical, one-time publications.

Nothing to Report

Other publications, conference papers, and presentations.

Nothing to Report

Website(s) or other Internet site(s)

Nothing to Report

Technologies or techniques

Nothing to Report

Inventions, patent applications, and/or licenses

Nothing to Report

Other Products

Nothing to Report

7. PARTICIPANTS & OTHER COLLABORATING ORGANIZATIONS

What individuals have worked on the project?

Provide the following information for: (1) PDs/PIs; and (2) each person who has worked at least one person month per year on the project during the reporting period, regardless of the source of compensation (a person month equals approximately 160 hours of effort). If information is unchanged from a previous submission, provide the name only and indicate "no change."

Name:	Michael Sano
Project Role:	Postdoctoral Fellow
Researcher Identifier (e.g. ORCID ID):	0000-0003-3823-5932
Nearest person month worked:	12
Contribution to Project:	Dr. Sano performed the work in the area of photoacoustic imaging, ultrasound probe development, and numerical simulations
Funding Support:	This award

Has there been a change in the active other support of the PD/PI(s) or senior/key personnel since the last reporting period?

No Change

What other organizations were involved as partners?

Nothing to report

8. SPECIAL REPORTING REQUIREMENTS

COLLABORATIVE AWARDS: *Nothing to report*

QUAD CHARTS: *Nothing to report*

APPENDICES: *Nothing to report*